







Broad Absorption Line Disappearance/Emergence in Multiple Ions in a Weak Emission-line Quasar

W. Yi^{1,2,3} , M. Vivek¹, W. N. Brandt^{1,4,5} , T. Wang⁶, J. Timlin¹, N. Filiz Ak^{7,8}, D. P. Schneider^{1,4}, J. P. U. Fynbo^{9,10} , Q. Ni¹, F. Vito^{11,12} , B. L. Indahl¹³, and Sameer¹

¹Department of Astronomy & Astrophysics, The Pennsylvania State University, 525 Davey Lab, University Park, PA 16802, USA

²Yunnan Observatories, Kunming, 650216, People's Republic of China

³Key Laboratory for the Structure and Evolution of Celestial Objects, Chinese Academy of Sciences, Kunming 650216, People's Republic of China

⁴Institute for Gravitation and the Cosmos, The Pennsylvania State University, University Park, PA 16802, USA

⁵Department of Physics, The Pennsylvania State University, University Park, PA 16802, USA

⁶CAS Key Laboratory for Research in Galaxies and Cosmology, Department of Astronomy, University of Science and Technology of China, People's Republic of China

⁷Faculty of Sciences, Department of Astronomy and Space Sciences, Erciyes University, 38039, Kayseri, Turkey

⁸Astronomy and Space Sciences Observatory and Research Center, Erciyes University, 38039, Kayseri, Turkey

⁹Cosmic Dawn Center (DAWN), Niels Bohr Institute, University of Copenhagen, Juliane Maries Vej 30, DK-2100 Copenhagen Ø, Denmark

¹⁰DTU-Space, Technical University of Denmark, Elektrovej 327, DK-2800 Kgs. Lyngby, Denmark

¹¹Instituto de Astrofísica and Centro de Astroingeniería, Facultad de Física, Pontificia Universidad Católica de Chile, Casilla 306, Santiago 22, Chile

¹²Chinese Academy of Sciences South America Center for Astronomy, National Astronomical Observatories, CAS, Beijing 100012, People's Republic of China

¹³Department of Astronomy, University of Texas, Austin, TX 78712, USA

Received 2018 November 26; revised 2019 January 4; accepted 2019 January 4; published 2019 January 15

Abstract

We report the discovery of the disappearance of Mg II, Al III, C IV, and Si IV broad absorption lines (BALs) at the same velocity ($0.07c$), accompanied by a new C IV BAL emerging at a higher velocity (up to $0.11c$), in the quasar J0827+4252 at $z = 2.038$. This is the first report of BAL disappearance (i) over Mg II, Al III, C IV, and Si IV ions and (ii) in a weak emission-line quasar (WLQ). The discovery is based on four spectra from the Sloan Digital Sky Survey and one follow-up spectrum from Hobby–Eberly Telescope/Low-Resolution Spectrograph-2. The simultaneous C IV BAL disappearance and emergence at different velocities, together with no variations in the Catalina Real-Time Transient Survey light curve, indicate that ionization changes in the absorbing material are unlikely to cause the observed BAL variability. Our analyses reveal that transverse motion is the most likely dominant driver of the BAL disappearance/emergence. Given the presence of mildly relativistic BAL outflows and an apparently large C IV emission-line blueshift that is likely associated with strong bulk outflows in this WLQ, J0827+4252 provides a notable opportunity to study extreme quasar winds and their potential in expelling material from inner to large-scale regions.

Key words: galaxies: active – quasars: absorption lines – quasars: individual (SDSS J0827+4252)

1. Introduction

Broad absorption line quasars (BALQSOs; Weymann et al. 1991) make up $\approx 15\%$ of quasars discovered to date (e.g., Trump et al. 2006; Gibson et al. 2009), but their intrinsic fraction may be up to $\approx 40\%$ due to selection effects (e.g., Allen et al. 2011). They are often classified as high-ionization BALQSOs (HiBALs) and low-ionization BALQSOs (LoBALs). HiBAL quasars show absorption features only from relatively high-ionization species such as C IV and Si IV. LoBAL quasars possess high-ionization features plus absorption from low-ionization species, typically Al III and Mg II. Almost all BALQSOs are characterized by blueshifted absorption troughs imprinted on their spectra, signaling outflows along our line of sight (LOS).

The inner circumnuclear regions of quasars cannot be spatially resolved with current technology, and thus we cannot directly observe the physical processes that cause BAL outflows. However, BAL variability provides one of the most powerful diagnostics for exploring the nature and origin of such outflows. Statistically, BAL variability is widely

explained by transverse motions of BAL absorbers across our LOS or ionization changes in response to continuum variations (e.g., Capellupo et al. 2011; Filiz Ak et al. 2013; Wang et al. 2015).

BAL emergence or disappearance, an extreme and relatively rare form of BAL variability, is often interpreted as gas moving into or out of our LOS (e.g., Junkkarinen et al. 2001; Hamann et al. 2008; Leighly et al. 2009; Krongold et al. 2010; Hall et al. 2011; Vivek et al. 2012; Rafiee et al. 2016). Some studies, however, report observational evidence in support of ionization changes (e.g., McGraw et al. 2017; Stern et al. 2017; Vivek et al. 2018). A few studies based on relatively large samples confirm that both the ionization-change and transverse-motion mechanisms account for most BAL emergence/disappearance phenomena (e.g., Filiz Ak et al. 2012; Wang et al. 2015; McGraw et al. 2017; De Cicco et al. 2018; Rogerson et al. 2018; Sameer et al. 2019). The dominant driver of BAL emergence/disappearance in individual BALQSOs, however, often remains uncertain due to a lack of sufficient observational evidence to break degeneracies inherent in BAL variability. In fact, BAL disappearance or emergence phenomena have been reported mostly for weak BAL troughs caused by a single ionized species. Only a few investigations have reported BAL emergence or disappearance occurring over multiple-ion BAL



Original content from this work may be used under the terms of the [Creative Commons Attribution 3.0 licence](https://creativecommons.org/licenses/by/3.0/). Any further distribution of this work must maintain attribution to the author(s) and the title of the work, journal citation and DOI.

Table 1
Spectroscopic Observations of J0827+4252

Instrument Name	Signal-to-noise Ratio (S/N)	Spectral Coverage (Å)	Integration Time (seconds)	Observation Date (MJD)
SDSS	5.1	3800–9200	9120	52266
SDSS	3.4	3800–9200	3503	54524
BOSS	6.8	3650–10400	4504	55513
BOSS	6.7	3650–10400	5400	57063
HET/LRS2	7.2	3700–7000	2700	58212

Note. The S/N values represent the average S/N at $1750 < \lambda_{\text{rest}} < 1800 \text{ \AA}$. All spectra have a similar spectral resolution ($R \approx 1800$) at $\lambda_{\text{obs}} = 4000 \text{ \AA}$.

troughs (e.g., Hamann et al. 2008; Filiz Ak et al. 2012; McGraw et al. 2017; De Cicco et al. 2018; Rogerson et al. 2018). To date, no BAL variability studies have reported a case where BAL disappearance occurred over all of the commonly observed Mg II, Al III, C IV, and Si IV ions at the same velocity.

Weak emission-line quasars (WLQs) are a notable “extreme” subset of the quasar population (e.g., Fan et al. 1999; Diamond-Stanic et al. 2009; Shemmer et al. 2010; Luo et al. 2015; Plotkin et al. 2015; Wu et al. 2015), although previous studies have not reached consensus on the detailed nature of WLQs. Recent WLQ studies, mainly from an X-ray perspective, broadly support a “shielding” scenario for WLQs that is associated with high Eddington ratios (e.g., Wu et al. 2012; Luo et al. 2015; Ni et al. 2018). Likewise, some BALQSO models also require a “shielding” mechanism by which high-energy photons are blocked from reaching the ultraviolet (UV)-absorbing clouds (e.g., Proga et al. 2000), although a dense outflow could have a sufficiently low ionization level itself without shielding (e.g., Hamann et al. 2013; Baskin et al. 2014). Regardless of specific models, both BALQSOs and WLQs appear to have high-velocity outflows driven by radiation pressure. Indeed, UV BALs often show high LOS velocities ($>0.03c$; e.g., Hamann et al. 2008; Vivek et al. 2012; Rogerson et al. 2016), while both BALQSOs and WLQs tend to have larger C IV broad emission-line (BEL) blueshifts than non-BAL quasars (e.g., Richards et al. 2011; Luo et al. 2015). However, previous WLQ studies were almost entirely based on non-BAL objects. In this context, studying BALs in WLQs is valuable for understanding the connection between the two quasar subsets.

In this Letter, we report the first discovery of a dramatic BAL disappearance over Mg II, Al III, C IV, and Si IV species at the same velocity ($\sim 0.07c$) followed by a new, stronger C IV BAL emerging at a higher velocity (up to $0.11c$) in a LoBAL WLQ, J082747.14+425241.1 (hereafter J0827+4252) at $z = 2.038$.

2. Observations and Data Reduction

J0827+4252 is a LoBAL quasar selected from our Mg II BAL quasar sample (W. Yi et al. 2019, in preparation) that is dedicated to the large-scale investigation of Mg II BAL variability using multi-epoch spectra from the Sloan Digital Sky Survey-I/II (SDSS; York et al. 2000) and the Baryon Oscillation Spectroscopic Survey of SDSS-III (BOSS; Eisenstein et al. 2011; Dawson et al. 2013). SDSS and BOSS are wide-field, large sky survey projects using the same dedicated 2.5 m telescope at the Apache Point Observatory, New Mexico

(Gunn et al. 2006; Smee et al. 2013). Spectra for this quasar were taken at four well-separated epochs (see Table 1), and the fully reduced spectra were retrieved directly from the SDSS data release 14 (DR14) archive. In our sample, we noticed that Mg II, Al III, C IV, and Si IV BALs at the same velocity completely disappeared in this source. Therefore, this quasar was ranked as the highest priority for subsequent spectroscopic observations.

We obtained additional spectra for this quasar using the blue arm of the Low-Resolution Spectrograph-2 (LRS2; Chonis et al. 2014) mounted on the Hobby–Eberly Telescope (HET; Ramsey et al. 1998) on 2018 April 4. The newly obtained spectroscopic data were processed with the LRS2 pipeline (Davis et al. 2018; B. H. Indahl et al. 2019, in preparation), which includes standard long-slit spectral extraction procedures, but does not yet include flux calibration. However, the lack of flux calibration for the HET/LRS2 spectra does not affect the identification and measurement of BAL features. To calibrate the flux of the HET/LRS2 spectrum, we first fit a low-order polynomial to the spectrum and then scaled the spectrum so that the polynomial fit matches the reddened power-law fit (see Section 3) for the BOSS spectrum at MJD = 55513. In this process, we assumed that the HET/LRS2 spectrum and the BOSS spectrum at MJD = 55513 have the same continuum flux.

For better visual clarity, we smooth all the raw spectra with a 25 pixel Savitzky–Golay filter window as shown in Figure 1. This smoothing does not affect the appearance of the broad emission/absorption lines.

3. Observational Results

The barely visible C IV broad emission line and weak C III] +Mg II emission features in the different spectroscopic epochs shown in Figure 1 illustrate the WLQ nature of this LoBAL quasar. The four different-ion BALs at the same velocity have the same velocity width, suggesting that they arise in the same absorbing material. Note that the Si IV troughs are located at the blue edge of the spectra and are associated with large uncertainties; thus, the detection of Si IV BALs is not as reliable as that of the other BALs.

3.1. Continuum Fits and Equivalent Width (EW) Measurements

We adopt a reddened power-law model to fit the global continuum using the Small Magellanic Cloud (SMC)-like reddening function from Pei (1992). This model was fit to regions of the spectra that were visually identified to be relatively free of emission and absorption features (1260–1350 Å, 1750–1800 Å, 2100–2250 Å, 3000–3100 Å). Spectral slope and reddening are then derived from the global fits. Because of the WLQ nature of this LoBAL quasar, we choose another WLQ, J0945+1009 at $z = 1.683$, from Plotkin et al. (2015) as a template to fit our spectra at different epochs by optimizing the SMC-like reddening and scaling factors. As a comparison, we also consider a model combining a non-BAL composite spectrum (Vanden Berk et al. 2001) as a template in combination with the same SMC-like reddening function to fit these spectra. The left panels of Figure 1 display all spectra of J0827+4252 obtained from SDSS and HET/LRS2 (adopting $z = 2.038 \pm 0.005$ from Hewett & Wild 2010). There is clear trend that the weak emission-line feature becomes increasingly evident from low- to high-ionization emission lines, as noted by Plotkin et al. (2015); in addition, the C IV emission-line

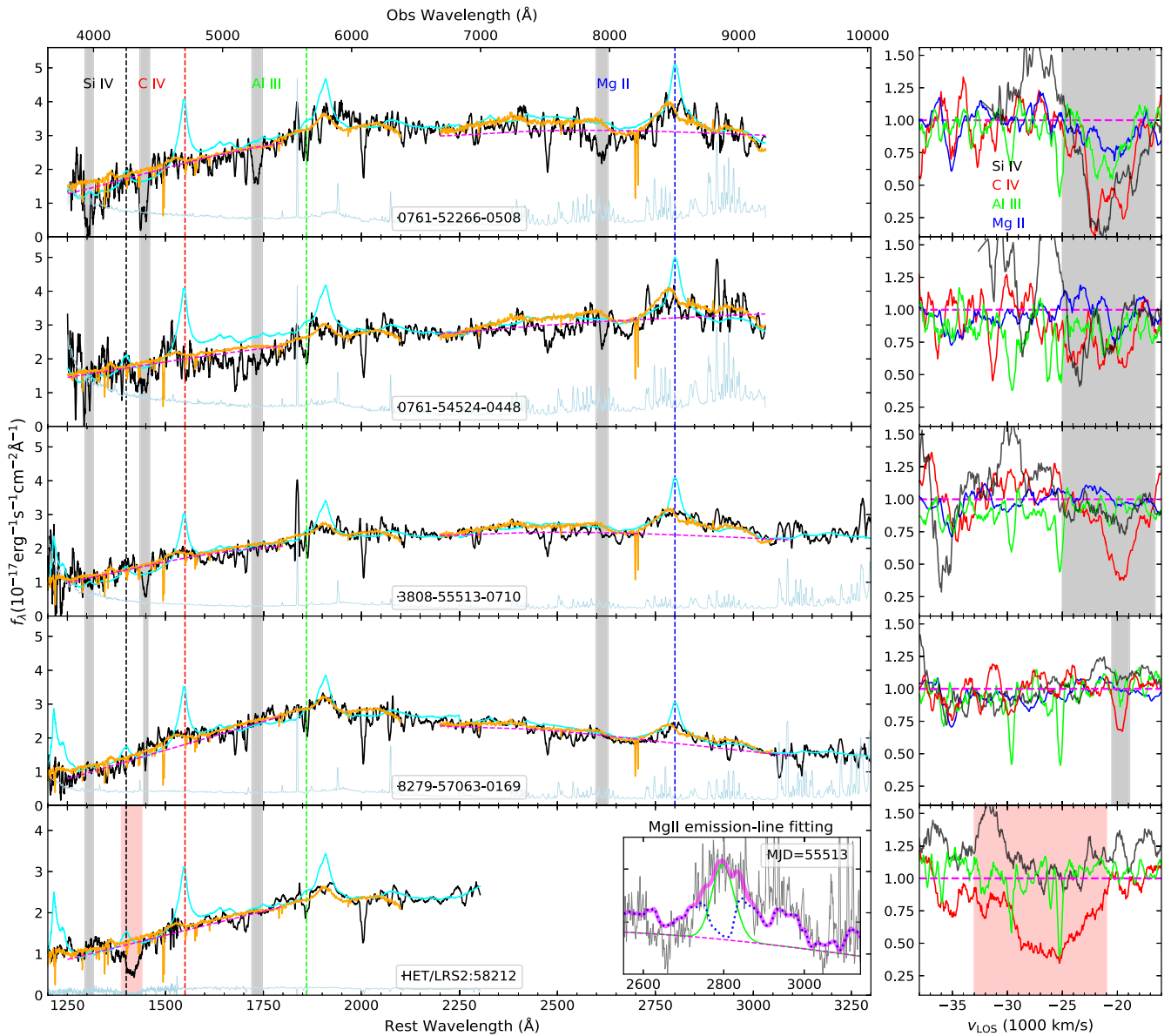


Figure 1. Left panels: different-epoch spectra with corresponding continuum (dashed magenta) and template fits using the composite template (cyan; Vanden Berk et al. 2001) and the WLQ spectrum of J0945+1009 (orange; Plotkin et al. 2015), respectively; gray shaded regions refer to four different-ion BALs and the red shaded region highlights the newly emerged C IV BAL. The blue, green, red, and black dashed vertical lines locate at 2800, 1860, 1550, and 1400 Å, respectively. Right panels: profiles of the four different-ion BALs (gray: Si IV, red: C IV, green: Al III, blue: Mg II) normalized by the local continuum fits in velocity space; dashed magenta horizontal lines represent the continuum level. The simultaneous C IV BAL disappearance/emergence occurs after MJD = 55513. The inset panel shows the spectral fit of the Mg II BEL at MJD = 55513 (the HET spectrum has no coverage at $\lambda_{\text{rest}} > 2300$ Å), in which the magenta line represents the best fit of the Mg II BEL using the same prescription as Shen et al. (2011), including a power-law continuum (dashed magenta), Fe II emission (dotted blue), and the Mg II BEL (green).

blueshift of J0827+4252 appears to be consistent with that of J0945+1009 (~ 5500 km s $^{-1}$). However, we require near-infrared (IR) spectroscopy to establish the C IV emission-line blueshift, as J0945+1009 does show dramatic Mg II emission-line blueshift compared to the systemic redshift determined by the H β emission line. As the global continuum fit may not be optimal for quantifying BAL properties, we choose the local continuum fit over these line-free regions using the same reddened power-law model for quantitative measurements. The local fits are in good agreement with global fits except for the spectrum at MJD = 57063, which has an apparent change in spectral shape possibly due to flux-calibration errors. To obtain BAL disappearance timescales over different ions, we do not consider the highly

uncertain spectrum at MJD = 54524 (S/N ~ 3 in the continuum). Using a 2σ EW measurement as the threshold of BAL trough detection, Mg II BAL disappeared by MJD = 55513, Si IV and Al III BALs disappeared by MJD = 57063, and the low-velocity C IV BAL disappeared by MJD = 58212. Our measurements of the spectra and BAL properties are tabulated in Table 2. The time evolution of the EWs of these BALs is shown in the bottom panel of Figure 2.

One conspicuous feature in Figure 2 is that the low-velocity C IV BAL slowly weakens until it completely disappears (over >5 yr in the rest frame), while a strong C IV BAL emerges abruptly (over <1 yr in the rest frame) at a higher velocity. Another dramatic feature is the faster disappearance of

Table 2
Measurements at Different Spectroscopic Epochs

MJD	52266	54524	55513	57063	58212
v_{LOS}^b	-23.2	-23.2	-23.2	-20.5	-33
v_{LOS}^r	-17.8	-17.8	-17.8	-18.8	-22
α_λ	-1.87	-1.1	-2.2	-4.97	-1.32
r	0.25	0.17	0.28	0.49	0.21
Mg II	6.3 ± 1.01	3.2 ± 1.15	0.6 ± 0.57	0.2 ± 0.45	
Al III	7.5 ± 0.65	4.3 ± 0.82	1.8 ± 0.43	0.1 ± 0.28	0
Si IV	13.5 ± 1.8	4.7 ± 4.8	3 ± 1.36	0 ± 0.53	0
C IV _l	13.2 ± 1.1	9.7 ± 1.75	8.9 ± 0.76	1.7 ± 0.76	0
C IV _h	0	0	0	1.2 ± 0.7	26 ± 0.7

Note. v_{LOS}^b and v_{LOS}^r are the blue- and red-edge velocities (1000 km s^{-1}) of each BAL trough. α_λ and r are the index and reddening derived from the global reddened power-law fits. The last five rows are the corresponding BAL EWs (\AA) over multiple ions at different epochs based on the local continuum fits, in which C IV_l and C IV_h represent the low-velocity and high-velocity C IV BALs, respectively.

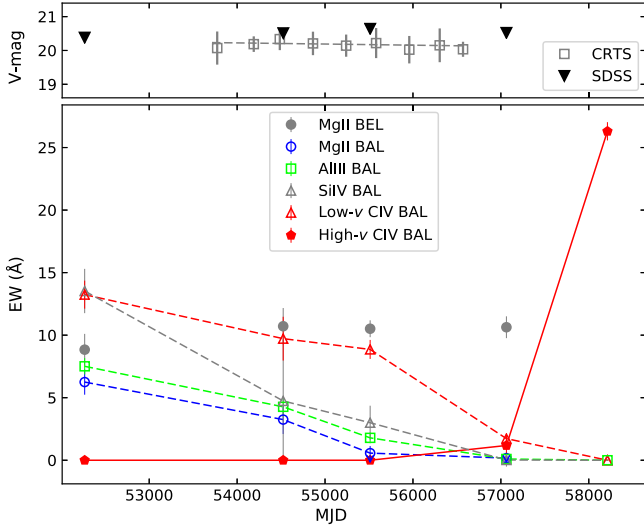


Figure 2. Top panel: the synthetic V-band light curve obtained from the Catalina Real-Time Transient Survey (CRTS), in which gray squares are mean values sampled within one-year intervals (the error bar is determined from the standard deviation in a corresponding interval). Inverted black triangles are the synthetic V-band magnitudes from different-epoch SDSS spectra. The dashed gray line represents the best linear fit. Bottom panel: MJD vs. BAL/BEL EW, in which C IV (red triangles), Si IV (gray triangles), Al III (green squares), and Mg II (blue circles) BALs are indicated. Downward arrows represent upper limits on EWs. The absolute Mg II BEL EWs are marked as filled gray dots. Red pentagons represent the newly emerged C IV BAL at a higher velocity compared to the disappearing C IV BAL.

LoBALs compared to HiBALs. These observational results provide diagnostics for investigating the dominant driver of the BAL disappearance/emergence and the structure of outflows (see Section 4).

3.2. Black Hole (BH) Mass Estimate

Based on the single-epoch virial relation, Shen et al. (2011) estimated the Mg II-based BH mass and Eddington ratio for this quasar to be $\sim 6.3 \times 10^9 M_\odot$ and $\lambda_{\text{Edd}} \sim 0.01$. Note that the Mg II-based BH mass from Shen et al. (2011) was measured from the spectrum at MJD = 52266 that has low S/N. We measured the Mg II BEL with a higher S/N spectrum at MJD = 55513 (see the inset panel of Figure 1)

using the same prescription from Shen et al. (2011), which yields a $\text{FWHM}_{\text{Mg II}} = 6990 \pm 610 \text{ km s}^{-1}$ after subtracting the power-law continuum and Fe II emission (see the dashed and dotted lines in the inset panel of Figure 1). Our measurement of the FWHM is consistent with that of Shen et al. (2011), where they measured $\text{FWHM}_{\text{Mg II}} = 8860 \pm 1340 \text{ km s}^{-1}$. The continuum fits indicate an approximately equal luminosity at 3000 \AA over the two epochs for this quasar (so $\log M_{\text{BH}} \propto \log \text{FWHM}^2$). Our measurement yields $M_{\text{BH}} \sim 4 \times 10^9 M_\odot$.

We caution that the uncertainties on the BH mass not only include measurement errors (~ 0.1 dex) and systematic errors (~ 0.3 – 0.5 dex) of the single-epoch scaling approach, but also may have additional systematic errors related to non-virial gas motions sometimes seen in WLQs (e.g., Plotkin et al. 2015).

4. Discussion

Ionization changes of BAL absorbers and transverse motions across our LOS are the two most widely accepted explanations accounting for BAL variability. We discuss these two possibilities in this section.

4.1. Ionization-change Scenario

Assuming solar abundances under an optically thin condition, the observed BAL disappearance over multiple ions can be explained by ionic column density variations in response to ionization changes. Depending on the initial value of the ionization parameter, a reduction in the column density of an ion can be caused by either an increase or a decrease in the ionizing flux. From Figure 4 of Hamann et al. (2001), the ionization parameter at MJD = 52266 can be constrained to be $\log U \sim -3$ due to the simultaneous presence of Mg II, Al III, C IV, and Si IV BALs. The subsequent disappearance of Mg II and Al III BAL troughs, together with the weakening of C IV and Si IV BALs by MJD = 55513, can be explained by an increase in the ionizing flux (to $\log U \sim -1.5$). The observations do not support a reduction in the ionizing flux, as the C IV BAL would have disappeared before the Mg II BAL in such a scenario. A continued increase in the ionizing flux would result in the further weakening and eventual disappearance of the low-velocity C IV BAL. However, the simultaneous disappearance of the low-velocity C IV BAL and appearance of the high-velocity C IV BAL at MJD = 58212 poses some problems. It is tempting to argue that the increase in the ionizing flux resulted in favorable ionization conditions for the C IV BAL to arise in high-velocity material at a larger distance. If the source of the ionizing flux is the same for the two absorbers, the fractional changes in the ionization parameter should be comparable for the two absorbers. However, the fractional ionization-parameter change required to explain the appearance of the high-velocity C IV BAL is much larger than that needed to explain the disappearance of the low-velocity C IV BAL.

The complete disappearance of the moderately strong low-velocity C IV BAL clearly requires a large change in the ionizing flux. Note that saturation in the absorption troughs (supported by the coexistence of Si IV, C IV, Al III, and Mg II BALs at the same velocity) demands an even larger change in the ionizing flux. Therefore, we likely expect to see variations in the UV light curve even though the actual ionizing photons are in the far-UV. To assess the UV continuum variability, we

analyzed the synthetic V -band light curve (corresponding to the UV band in the rest frame) obtained from the Catalina Real-Time Transient Survey (CRTS; Drake et al. 2009), as depicted in the top panel of Figure 2. As we are interested in the long-term continuum variability, we binned the light curve in one-year intervals (the grey squares). As a comparison, we also show the upper limit (due to possible flux missing from the spectroscopic aperture) on the V -band magnitudes (inverted black triangles in the top panel of Figure 2) derived from the SDSS spectra using the prescription from Jester et al. (2005). Both of the V -band light curves do not point to any significant changes in the continuum flux. Additionally, the EW measurements of the Mg II BEL ($2780 < \lambda_{\text{rest}} < 2820 \text{ \AA}$) indicate that the Mg II BEL did not experience substantial variations (see filled grey dots in the bottom panel of Figure 2) during our observations.

We also explored the radiation pressure confinement (RPC) model of Baskin et al. (2014), which proposes a radial density profile, leading to a range of U in a single-absorber system. Given the exponentially increasing density profile (Equation (22) of Baskin et al. 2014), the high-density, low- U gas (where the Mg II ions are formed) should be less sensitive to changes in the ionizing flux as compared to the low-density, high- U gas (where the C IV ions are formed). Therefore, ionization changes in the context of the RPC model are unlikely to explain our observation of faster disappearance of LoBAL troughs.

In light of the observational evidence discussed above, we conclude that the ionization-change mechanism is not a dominant driver of the BAL disappearance/emergence, although it may play a role in a single “direction” (BAL disappearance or BAL emergence).

4.2. Absorbing-gas Motion Scenario

We first assess the possibility of an accelerating BAL absorber moving from low to high velocity along our LOS. We did not find any monolithic shifts of the C IV BAL before its disappearance, and there are no Al III BAL (see Figure 1) appearing at a similar velocity as the newly emerged C IV BAL. Additionally, if the emerging C IV BAL were caused by the acceleration of the disappearing BAL, then the derived acceleration ($\approx 25 \text{ cm s}^{-2}$) would be about two orders of magnitude larger than the typical upper limit of BAL acceleration found in previous studies (e.g., Grier et al. 2016). Therefore, the acceleration of outflows along our LOS can be ruled out.

Next, we examine the case where BAL material moves across our LOS. In reality, a BAL absorber system may be composed of numerous “clouds” with a small volume filling factor (e.g., Hamann et al. 2013), and the BAL absorber density, as well as the background source emission, are most likely inhomogeneous. For simplicity, we consider a single cloud with a uniform density along our LOS. The BAL disappearance/emergence can be explained by a scenario in which one gas cloud containing both HiBAL/LoBAL absorbers takes more than five years to move out of our LOS; then, another cloud producing only C IV absorption spends less than one year moving into our LOS. The faster disappearance of the LoBALs can be explained if the low-ionization gas is embedded inside the high-ionization gas and has a smaller covering factor (e.g., Arav et al. 1999; Baskin et al. 2014). Observationally, such an explanation is supported by a recent study from Hamann et al. (2018), where they found

that low-ionization/high-column gas tends to have smaller covering fractions in BAL outflows based on a large BALQSO sample. No Al III BAL appears at a similar velocity to the emerging C IV BAL in the HET spectrum. This could be due to either the low-ionization gas not yet moving into our LOS or the material associated with the emerging C IV BAL having a relatively high level of ionization.

To estimate the continuum source size, we choose the Mg II-based BH mass ($4 \times 10^9 M_{\odot}$) of this quasar (see Section 3.2). Following Rogerson et al. (2016), the lower limit on the projected size of the continuum region is estimated to be $\sim 0.01 \text{ pc}$. The average trough depth (~ 0.6) of the disappearing C IV BAL indicates that the BAL absorber covers at least 60% of the projected area of the continuum source. To set a lower limit on the transverse velocity (see Rogerson et al. 2016 for details), we consider the homogeneous, sharp-edged case where $D_t = f \times D_b$ (D_t , f , and D_b refer to the crossing distance, LOS covering factor, and the projected size of the background source, respectively). The lower limit on the transverse velocity is estimated to be $v_t > 1100 \text{ km s}^{-1}$ using the BAL disappearance timescale (5.36 yr). As a comparison, the mean radial LOS velocity of the disappearing C IV BAL is $20,000 \text{ km s}^{-1}$. If we assume that the transverse velocity is comparable to the Keplerian velocity (see, e.g., McGraw et al. 2017), then the derived distance between the absorber and the central engine is 14.2 pc .

For the newly emerged C IV BAL at $v_{\text{LOS}} \sim 0.1c$, a lower limit on the transverse velocity is derived to be 5870 km s^{-1} using the change of trough depth (~ 0.6) and BAL emergence timescale ($< 1 \text{ yr}$). Similarly, the derived distance between the absorber and the central engine is less than 0.5 pc , assuming the Keplerian velocity. We require follow-up spectroscopy to trace a time evolution (at least the whole emerging process) for the newly emerged BAL trough and obtain a better estimate of BH mass. This in turn can be used to derive an upper limit on the transverse velocity and constrain its ionization level as well as outflow structure to the low-velocity BAL absorber.

5. Summary and Future Work

We report a case of BAL disappearance/emergence in a WLQ for the first time, where LoBALs at the same velocity disappeared faster than HiBALs, followed by a quick emergence of a strong C IV BAL at a higher velocity. Based on the simultaneous BAL disappearance/emergence and non-variability of the continuum flux, we disfavor a scenario where an ionization change in the absorbing material resulted in the observed BAL variability. Transverse motion of the absorption system is the most likely dominant driver of BAL disappearance/emergence for this quasar.

Such dramatic BAL disappearance over multiple ions, the quick emergence of a strong BAL trough, and the presence of mildly relativistic outflows in this WLQ, together suggest an extreme, wind-dominated phase, in which BAL absorbers are expected to cross our LOS more quickly and frequently than in other BAL quasars. Multi-wavelength follow-up observations will be helpful for further investigations regarding physical properties of the WLQ, the connection between WLQs and BALQSOs, the relative roles of BAL/BEL outflows and their potential in expelling material from inner to large-scale regions. Particularly, UV/optical/near-IR follow-up spectroscopy will allow us to establish the C IV-BEL blueshift, trace subsequent BAL/BEL variability (possible LoBAL emergence), and

obtain a better estimate of the BH mass, which is critical for probing the physical nature of this LoBAL WLQ.





We thank Michael Eracleous, Xiaohui Fan, and Patrick Hall for stimulating discussions. We thank Richard Plotkin for kindly providing the WLQ spectra of J0945+1009 obtained by VLT/X-shooter. We are grateful to Robin Ciardullo and Michael Eracleous for assistance with the observations by the Hobby–Eberly Telescope. We thank Xiaohui Fan, Jonathan Trump, Feige Wang, and Jinyi Yang for help in preparing follow-up observations.

W. Yi thanks financial support from the China Scholarships Council (No. 201604910001) for his postdoctoral study at the Pennsylvania State University. W. Yi also thanks support from the Chinese National Science Foundation (NSFC-11703076) and the West Light Foundation of The Chinese Academy of Sciences (Y6XB016001). M.V. and W.N.B. acknowledge support from NSF grant AST-1516784. J.T. acknowledges support from NASA ADP grant 80NSSC18K0878. N.F.A. thanks TUBITAK (115F037) for financial support. F.V. acknowledges financial support from CONICYT and CASSACA through the Fourth call for tenders of the CAS-CONICYT Fund. The Cosmic Dawn Center is funded by the DNRF.

Funding for SDSS-III has been provided by the Alfred P. Sloan Foundation, the Participating Institutions, the National Science Foundation, and the U.S. Department of Energy Office of Science. The Low-Resolution Spectrograph-2 (LRS2) was developed and funded by the University of Texas at Austin McDonald Observatory and Department of Astronomy, and by the Pennsylvania State University. We thank the Leibniz-Institut für Astrophysik Potsdam and the Institut für Astrophysik Göttingen for their contributions to the construction of the integral field units.

The Hobby–Eberly Telescope (HET) is a joint project of the University of Texas at Austin, the Pennsylvania State University, Ludwig-Maximilians-Universität München, and Georg-August-Universität Göttingen. The Hobby–Eberly Telescope is named in honor of its principal benefactors, William P. Hobby and Robert E. Eberly.

ORCID iDs

W. Yi  <https://orcid.org/0000-0001-9314-0552>
 W. N. Brandt  <https://orcid.org/0000-0002-0167-2453>
 J. P. U. Fynbo  <https://orcid.org/0000-0002-8149-8298>
 F. Vito  <https://orcid.org/0000-0003-0680-9305>

References

- Arav, N., Korista, K. T., de Kool, M., et al. 1999, *ApJ*, 516, 27
 Allen, J. T., Hewett, P. C., Maddox, N., et al. 2011, *MNRAS*, 410, 860
 Baskin, A., Laor, A., & Stern, J. 2014, *MNRAS*, 445, 3025
 Capellupo, D. M., Hamann, F., Shields, J. C., et al. 2011, *MNRAS*, 413, 908
 Chonis, T. S., Hill, G. J., Lee, H., et al. 2014, *SPIE*, 9147, 91470A
 Davis, B. D., Ciardullo, R., Jacoby, G. H., et al. 2018, *ApJ*, 863, 189
 Dawson, K. S., Schlegel, D. J., Ahn, C. P., et al. 2013, *AJ*, 145, 10
 De Cicco, D., Brandt, W. N., Grier, C. J., et al. 2018, *A&A*, 616, 114
 Diamond-Stanic, A. M., Fan, X., Brandt, W. N., et al. 2009, *ApJ*, 699, 782
 Drake, A. J., Djorgovski, S. G., Mahabal, A., et al. 2009, *ApJ*, 696, 870
 Eisenstein, D. J., Weinberg, D. H., Agol, E., et al. 2011, *AJ*, 142, 72
 Fan, X., Strauss, M. A., Gunn, J. E., et al. 1999, *ApJ*, 526, 57
 Filiz Ak, N., Brandt, W. N., Hall, P. B., et al. 2012, *ApJ*, 757, 114
 Filiz Ak, N., Brandt, W. N., Hall, P. B., et al. 2013, *ApJ*, 777, 168
 Gibson, R. R., Jiang, L., Brandt, W. N., et al. 2009, *ApJ*, 692, 758
 Grier, C. J., Brandt, W. N., Hall, P. B., et al. 2016, *ApJ*, 824, 130
 Gunn, J. E., Siegmund, W. A., Mannery, E. J., et al. 2006, *AJ*, 131, 2332
 Hall, P. B., Anosov, K., White, R. L., et al. 2011, *MNRAS*, 411, 2653
 Hamann, F., Barlow, T. A., Chaffee, F. C., et al. 2001, *ApJ*, 550, 142
 Hamann, F., Chartas, G., McGraw, S., et al. 2013, *MNRAS*, 435, 133
 Hamann, F., Herbst, H., Paris, I., et al. 2018, arXiv:1810.03686
 Hamann, F., Rodríguez Hidalgo, P., Prochaska, J. X., et al. 2008, *MNRAS*, 391, 39
 Hewett, P. C., & Wild, V. 2010, *MNRAS*, 405, 2302
 Jester, S., Schneider, D. P., Richards, G. T., et al. 2005, *ApJ*, 130, 873
 Junkkarinen, V., Shields, G. A., Beaver, E. A., et al. 2001, *ApJL*, 549, L155
 Krongold, Y., Binette, L., Hernández-Ibarra, F., et al. 2010, *ApJ*, 724, 203
 Leighly, K. M., Hamann, F., Casebeer, D. A., et al. 2009, *ApJ*, 701, 176
 Luo, B., Brandt, W. N., Hall, P. B., et al. 2015, *ApJ*, 805, 122
 McGraw, S. M., Brandt, W. N., Grier, C. J., et al. 2017, *MNRAS*, 469, 3163
 Ni, Q., Brandt, W. N., Luo, B., et al. 2018, *MNRAS*, 480, 5184
 Pei Yichuan, C. 1992, *ApJ*, 395, 130
 Plotkin, R. M., Shemmer, O., Trakhtenbrot, B., et al. 2015, *ApJ*, 805, 123
 Proga, D., Stone, J. M., & Kallman, T. R. 2000, *ApJ*, 543, 686
 Rafiee, A., Pirkola, P., Hall, P. B., et al. 2016, *MNRAS*, 459, 2472
 Ramsey, L. W., Adams, M. T., Barnes, T. G., et al. 1998, *Proc. SPIE*, 3352, 34
 Richards, G. T., Kruczek, N. E., Gallagher, S. C., et al. 2011, *AJ*, 141, 167
 Rogerson, J. A., Hall, P. B., Ahmed, N. S., et al. 2018, *ApJ*, 862, 22
 Rogerson, J. A., Hall, P. B., Rodríguez Hidalgo, P., et al. 2016, *MNRAS*, 457, 405
 Sameer, Brandt, W. N., Anderson, S., et al. 2019, *MNRAS*, 482, 1121
 Shemmer, O., Trakhtenbrot, B., Anderson, S. F., et al. 2010, *ApJ*, 722, 152
 Shen, Y., Richards, G. T., Strauss, M. A., et al. 2011, *ApJS*, 194, 45
 Smee, S. A., Gunn, J. E., Uomoto, A., et al. 2013, *ApJ*, 146, 32
 Stern, D., Graham, M. J., Arav, N., et al. 2017, *ApJ*, 839, 106
 Trump, J. R., Hall, P. B., Reichard, T. A., et al. 2006, *ApJS*, 165, 1
 Vanden Berk, D. E., Richards, G. T., Bauer, A., et al. 2001, *AJ*, 122, 549
 Vivek, M., Srianand, R., Dawson, K. S., et al. 2018, *MNRAS*, 481, 5570
 Vivek, M., Srianand, R., Mahabal, A., et al. 2012, *MNRAS*, 421, 107
 Wang, T., Yang, C., Wang, H., et al. 2015, *ApJ*, 814, 150
 Weymann, R. J., Morris, S. L., Foltz, C. B., et al. 1991, *ApJ*, 373, 23
 Wu, J., Brandt, W. N., Anderson, S. F., et al. 2012, *ApJ*, 747, 10
 Wu, X.-B., Wang, F., Fan, X., et al. 2015, *Natur*, 518, 512
 York, D. J., Adelman, J., Anderson, J. E., et al. 2000, *AJ*, 120, 1579